IFS #654

July 8, 1994

Isotope scaling and η_i mode with impurities in tokamak plasmas

J.Q. Dong*, W. Horton, and W. Dorland
Institute for Fusion Studies, The University of Texas at Austin
Austin, Texas 78712

The ion temperature gradient (ITG) driven instability, or η_i mode, is studied for discharges with hydrogen, deuterium or tritium in a toroidal magnetic configuration. Impurity effects on the mode and the instability (impurity mode) driven by presence of impurity ions with negative density gradient are studied. It is found that the maximum growth rate of the η_i mode scales as $M_i^{-1/2}$ for pure hydrogenic plasmas, where M_i is the mass number of the working gas ion. With the inclusion of impurity ions, the growth rate of the η_i mode decreases in all three kinds of plasmas with a hydrogen plasma still having the highest maximum growth rate, tritium the lowest, and deuterium in between. However, the isotope effects are weaker and scale as $M_{\rm eff}^{-1/2}$ with the presence of impurity ions, where the effective mass number $M_{\rm eff} = (1-f_z)M_i + f_z M_z$ with M_z and $f_z = \frac{Zn_{0z}}{n_{0e}}$ being the mass number and charge concentration of impurity ions, respectively. For the impurity mode the scaling is similar to that of the η_i mode without impurity ions. The experimental database shows that the plasma energy confinement time scales as $\tau_E \propto M_i^{1/2}$ for a wide range of clean plasmas. The correlation of the theoretical results with the experimental confinement scaling is discussed.

*Permanent address: Southwestern Institute of Physics, Chengdu, China

I. INTRODUCTION

Obtaining and understanding scaling laws for the energy confinement time in tokamak plasmas have long been a focus of experimental and theoretical studies in fusion plasma physics. Several empirical scaling laws have been proposed and work well for low (L) mode and high (H) mode discharges.[1,2,3] One of the common features of these scaling laws is that the plasma energy confinement time $\tau_E \propto M_i^\alpha$, where M_i is the hydrogenic ion mass number and $0.3 < \alpha < 0.7$ is a constant that varies from one scaling law to another. This τ_E versus M_i^α scaling is called the isotope scaling or isotope effects. Recently, the results of a wide range of studies about the isotope scaling performed on the Axisymmetric Divertor Experiment (ASDEX) as well as on other tokamak devices were reported and a variety of isotope scaling laws obtained from experiments summarized.[3] Despite its fundamental nature and widespread appearance in the experimental observations, theoretical explanations for the isotope scaling are rare. Moreover, conventional transport theories usually fail in predicting the right isotope scaling. Neoclassical theory, conventional ion pressure gradient driven turbulence models and resistive ballooning theory, for instance, predict a degradation of confinement from hydrogen to deuterium.

Theoretical attempts have been made to overcome the contradiction between experiments and theories. Impurity ion species are introduced into the ion temperature gradient (ITG) mode turbulence, which is widely believed to be responsible for anomalous energy transport in tokamak plasmas, to make M_i an explicit parameter in the transport properties.[4–6] In addition, the impurity mode, that is driven unstable by the presence of second ion species with negative density gradient even without an ion temperature gradient, is considered to account for the energy transport in plasma periphery.[5,6] A slab magnetic configuration is used and even a simplified local dispersion equation valid for long wavelength approximation in a shearless slab geometry is solved in these earlier studies.

A more complete toroidal equation including ion curvature and magnetic gradient drift motions needs to be solved in this regard since the growth rate and the structure of the mode depend on the toroidal drifts of the ions and the toroidicity of magnetic configuration. Models based on the collisional drift wave turbulence in a region with magnetic shear seem to catch the right trends.[7] However, collisionless plasma dynamics is more relevant to high temperature core plasmas in tokamak devices.

The impurity effects on ITG (or η_i) mode in collisionless plasmas are studied for shearless slab, shear slab and toroidal magnetic configurations in Ref. 8. Full hydrogen and impurity ion dynamics are taken into account and the ballooning representation is used to take care of the linear mode coupling introduced by the toroidicity of the tokamak plasmas. The same integral dispersion equation for toroidal drift modes is used to study the isotope effects on ITG and impurity driven modes as well as on plasma confinement in this work.

The remainder of this work is organized as follows. In Sec. II the integral dispersion equation, including a second ion species, for toroidal plasmas is presented and explained briefly for completeness. In Sec. III the numerical results for hydrogenic plasmas, with and without impurity species, are described. Both the ITG and impurity modes are studied in the former case. A possible correlation of these results with experimentally observed isotope scaling is discussed in Sec. VI. Sec. V is devoted to the conclusions of this study.

II. INTEGRAL DISPERSION EQUATION

The gyrokinetic integral equation[9] for the study of low frequency drift modes, such as the ITG mode, is extended to include impurity species in this section. The curvature and magnetic gradient effects $\omega_D(v_\perp^2, v_\parallel^2, \theta)$ of both hydrogenic and impurity ions are included. The ballooning representation is used so that the linear mode coupling due to the toroidal magnetic configuration of tokamak device is taken into account. The full ion transit $k_\parallel v_\parallel$ and finite Larmor radius effects are retained while the ion bouncing is neglected. The electron

response is assumed to be adiabatic for simplicity. The integral dispersion equation derived in Ref. 9 is easily written as follows after being extended to include second ion species,

$$[1+\tau_i(1-f_z)+\tau_z Z f_z]\,\widehat{\phi}(k)=\int_{-\infty}^{+\infty}\frac{dk'}{\sqrt{2\pi}}K(k,k')\widehat{\phi}(k')\ , \tag{1}$$

where

$$K(k,k')=-i\int_{-\infty}^{0}\omega_{*e}d\tau\,\sqrt{2}\,e^{-i\omega\tau}\Bigg[(1-f_z)\frac{\exp\left[-\frac{(k'-k)^2}{4\lambda}\right]}{\sqrt{a}\,(1+a)\sqrt{\lambda}}$$

$$\times\Bigg\{\frac{\omega}{\omega_{*e}}\tau_i+L_{ei}-\frac{3}{2}\eta_i L_{ei}+\frac{2\eta_i L_{ei}}{(1+a)}$$

$$\times\left[1-\frac{k_\perp^2+k'^2}{2(1+a)\tau_i}+\frac{k_\perp\,k'_\perp}{(1+a)\tau_i}\frac{I_1}{I_0}\right]+\frac{\eta_i L_{ei}(k-k')^2}{4a\lambda}\Bigg\}\Gamma_0(k_\perp,k'_\perp)$$

$$+f_z\frac{\exp\left[-\frac{(k'-k)^2}{4\lambda_z}\right]}{\sqrt{a}_z\,(1+a_z)\sqrt{\lambda_z}}\Bigg\{\frac{\omega}{\omega_{*e}}Z\tau_z+L_{ez}-\frac{3}{2}\eta_z L_{ez}+\frac{2\eta_z L_{ez}}{(1+a_z)}$$

$$\times\left[1-\frac{(k_\perp^2+k'^2)\mu}{2(1+a_z)Z^2\tau_z}+\frac{k_\perp\,k'_\perp\mu}{(1+a_z)Z^2\tau_z}\frac{I_{1z}}{I_{0z}}\right]+\frac{\eta_z L_{ez}(k-k')^2}{4a_z\lambda_z}\Bigg\}\Gamma_{0z}(k_\perp,k'_\perp)\Bigg] \tag{2}$$

with

$$\lambda=\frac{\tau^2\omega_{*e}^2}{\tau_i a}\left(\frac{\widehat{s}}{q}\epsilon_n\right)^2\ ,\quad \lambda_z=\frac{\tau^2\omega_{*e}^2}{\tau_z a_z\mu}\left(\frac{\widehat{s}}{q}\epsilon_n\right)^2\ ,$$

$$a=1+\frac{i2\epsilon_n}{\tau_i}\omega_{*e}\tau\left(\frac{(\widehat{s}+1)(\sin\theta-\sin\theta')-\widehat{s}(\theta\cos\theta-\theta'\cos\theta')}{(\theta-\theta')}\right)\ ,$$

$$a_z=1+\frac{i2\epsilon_n}{\tau_z Z}\omega_{*e}\tau\left(\frac{(\widehat{s}+1)(\sin\theta-\sin\theta')-\widehat{s}(\theta\cos\theta-\theta'\cos\theta')}{(\theta-\theta')}\right)\ ,$$

$$\theta=\frac{k}{\widehat{s}k_\theta}\ ,\quad \theta'=\frac{k'}{\widehat{s}k_\theta}\ ,$$

$$\Gamma_0 = I_0\left(\frac{k_\perp k'_\perp}{(1+a)\tau_i}\right)\exp\left[-(k_\perp^2+k'^2_\perp)/2\tau_i(1+a)\right]$$

$$\Gamma_{0z} = I_0\left(\frac{k_\perp k'_\perp \mu}{(1+a_z)\tau_z Z^2}\right)\exp\left[-(k_\perp^2+k'^2_\perp)\mu/2Z^2\tau_z(1+a_z)\right] ,$$

$$k_\perp^2 = k_\theta^2 + k^2 , \qquad k'^2_\perp = k_\theta^2 + k'^2 ,$$

$$\epsilon_n = \frac{L_{ne}}{R} , \quad \eta_i = \frac{L_{ni}}{L_{Ti}} , \quad \eta_z = \frac{L_{nz}}{L_{Tz}} , \quad \tau_i = \frac{T_e}{T_i} , \quad \tau_z = \frac{T_e}{T_z} ,$$

$$f_z = \frac{Zn_{0z}}{n_{0e}} , \quad \mu = \frac{m_z}{m_i} , \quad L_{ei} = \frac{L_{ne}}{L_{ni}} , \quad L_{ez} = \frac{L_{ne}}{L_{nz}} .$$

The quantities k, k' and k_θ are normalized to $\rho_i^{-1} = \Omega_i/v_{ti} = eB/c\sqrt{2T_i m_i}$, x is normalized to ρ_i, and $I_j(j=0,1)$ is the modified Bessel function of order j. The symbols with subscript "i" or without stand for the primary ion species (hydrogenic ions) while that with "z" and "e" stand for the second ion species and electrons, respectively, throughout this paper.

In addition, all the symbols have their usual meanings such as the L_n's are the density scale lengths, n_0's are the unperturbed densities, L_T's are the temperature scale lengths, q is the safety factor, $\hat{s} = rdq/qdr$ is the magnetic shear and $\omega_{*e} = ck_\theta T_e/eBL_{ne}$ is the electron diamagnetic drift frequency. Z is the charge number of impurity ions, m's and T's are the species' mass and temperature, respectively. The derivation and detailed explanation of the equation are given in Ref. 9 and not repeated here.

It has to be mentioned before starting to solve Eq. (1) that not all the parameters are independent. This is because that the quasineutrality condition holds in the plasmas studied here. This condition requires that

$$L_{ei} = \frac{1 - f_z L_{ez}}{1 - f_z} , \tag{3}$$

and therefore

$$\eta_z = \frac{\eta_i(\frac{L_{nz}}{L_{ne}} - f_z)}{(1 - f_z)}\ , \tag{4}$$

under the assumption $T_i(r) = T_z(r)$.

III. NUMERICAL RESULTS

Equation (1) has to be solved numerically and special attention must be paid to the logarithmic singularity at $\tau = 0$ when $k = k'$.[9] The numerical methods for solving such a Fredholm integral equation of second kind are standard and well documented[9] so will not be repeated in this work.

The following reference parameters are used in this study unless otherwise stated, $\eta_i = \eta_z = 3.9$, $f_z = 0.2$, $\hat{s} = 0.83$, $q = 1.5$, $\epsilon_n = 0.56$, $\tau_i = \tau_z = 1$, $L_{ei} = L_{ez} = 1$.

A. ITG mode in pure hydrogenic plasmas

The ITG mode in pure hydrogen (H), deuterium (D), tritium (T) or their mixture plasmas is studied first to show the isotope effects on the mode. The normalized mode growth rate as a function of $k_\theta \rho_H$ is given in Fig. 1, where $\rho_H = c\sqrt{2T_i m_H}/eB$ is the hydrogen ion Larmor radius. The mode growth rate is normalized to $\omega_{*e}/k_\theta \rho_H = \sqrt{\tau_i/2}c_{sH}/L_{ne}$ so that the normalized growth rate is independent of the poloidal mode number k_θ which is the variable on the abscissa axis. With this uniform normalization, the results obtained for the various species may be directly compared.

The results shown in Fig. 1 make it very clear that the ITG mode has the highest maximum growth rate and the widest k_θ range where the mode is unstable in a hydrogen plasma. Tritium plasma has the lowest maximum growth rate and the narrowest unstable k_θ range and is thus the most stable. A deuterium plasma is in between. The stability of the ITG mode in a half and half D-T plasma is just between the stabilities of deuterium

and tritium plasmas, and the similar for a half and half H-D plasmas. It is easy to figure out that the maximum growth rates $\gamma_{\mathrm{max}H} : \gamma_{\mathrm{max}D} : \gamma_{\mathrm{max}T} = 1 : 1/\sqrt{2} : 1/\sqrt{3}$, i.e. the maximum growth rate of the mode is inversely proportional to the square root of the ion mass number. This relation holds for D-T and H-D mixing plasmas if an average mass number $\overline{M} = \sum_i \frac{n_{0i}M_i}{n_{0e}}$ is used. A possible correlation of these results with isotope scaling of energy confinement in tokamak plasmas will be discussed in Sec. IV.

B. ITG mode in plasmas with impurities

Real plasmas in tokamak devices are not pure hydrogenic plasmas. Instead, there are impurities in such plasmas. A second ion species is introduced in order to study the isotope effects on ITG mode in the presence of impurities. Two kinds of impurities, carbon and helium, are considered. Shown in Fig. 2 is the normalized mode growth rate as a function of poloidal wave number. The same normalization as that in Fig. 1 is used. In both carbon and helium cases the impurity charge concentration $f_z = Zn_{0z}/n_{0e} = 0.2$ is used, corresponding to $Z_{\mathrm{eff}} = 2$ with carbon and $Z_{\mathrm{eff}} = 1.2$ with helium, respectively. Again, the mode has the highest maximum growth rate in a hydrogen plasma, the lowest in a tritium, and the intermediate in a deuterium plasma. In addition, the mode growth rate in plasmas with carbon is lower than that with helium when the primary ions are same kind (H, D, or T).

C. Impurity mode

Impurity mode can be driven unstable only when there is a second ion species in the plasma and its density peaks opposite to the primary ion and electron densities.[10] With opposing density gradients, no ion temperature gradient is needed to drive this instability. We choose $\eta_i = \eta_z = 0$, $L_{ne} = -2L_{nz}$, $\hat{s} = 1$, $q = 2.5$, $\epsilon_n = 0.3$. The parameter $L_{ei} = L_{ne}/L_{ni}$ is calculated from Eq. (3). Oxygen is considered to be the impurity in hydrogen, deuterium or tritium plasmas. Shown in Fig. 3 is the mode growth rate as a function of the wave

number in the poloidal direction. Two impurity charge concentrations of $f_z = 0.2$ and 0.3 ($Z_{\rm eff} = 2.4$ and 3.1) are studied in Figs. 3(a)–(b), respectively. In these two cases the mode growth rate is the highest in a hydrogen plasma, the lowest in a tritium, and the intermediate in a deuterium plasma. In addition, the mode has widest range of unstable k_θ in a hydrogen plasma, narrowest in a tritium, and the intermediate in a deuterium plasma, just as the ITG mode does. The mode growth rate increases with increasing impurity concentration for same discharge gas in the range of parameters studied here.

IV. DISCUSSION

It is widely believed that ITG mode is a plausible candidate responsible for the anomalous energy transport in tokamak plasmas.[4,5,11] There has been an effort to explain experimental observations with ITG theories.[11] As one part of such effort it is natural to try to find a possible relationship between the ITG mode features and experimental observations on the isotope scaling. The mixing length argument, $\chi \simeq \gamma \Delta_r^2$, is usually used to calculate the thermal diffusivity χ induced by plasma microinstabilities, where γ is the linear mode growth rate and Δ_r is the mode correlation length in the radial direction. The conventional estimate identifies Δ_r with the mode width of a single harmonic and takes $\Delta_r \sim k_\theta^{-1}$ the order of ion gyroradius. Such estimation gives rise to two important discrepancies with the experiments. The first is the radial profile of $\chi(r)$. Such calculations always underestimate the transport in cold region of plasma column (near the edge). The reason for this is that k_θ^{-1} and γ are normalized to $\rho_s = c\sqrt{T_e m_i}/eB$ and $c_s/L_n = \sqrt{T_e/m_i}/L_n$, respectively, and their numbers are independent of parameters such as ion mass m_i, temperature $T = T_i = T_e$ and magnetic field intensity B in these normalizations. This leads to so-called gyroBohm scaling $\chi \propto T^{3/2}/B^2$ of the theoretical plasma heat conductivity with temperature T and magnetic field intensity B in the mixing length estimation. This scaling makes χ drop towards plasma boundary due to decreasing temperature, while actual experimental transport

usually increases towards plasma edge. This issue has been discussed by Beklemishev and Horton.[12] The second is the isotope scaling of the energy diffusion coefficient. Based on exactly the same argument given above, the conventional mixing length estimation results in the isotope scaling $\chi \propto M_i^{1/2}$ that is contrary to the experimental observation $\chi \propto M_i^{-1/2}$.

Recent gyrokinetic and particle simulations of ITG driven instabilities show that the radial correlation length is longer than and does not scale directly with $1/k_\theta$, and that radially elongated ballooning mode structure is a common characteristic of two-dimensional linear eigenmode and nonlinear turbulence in a toroidal configuration.[13–15] Indeed, an electrostatic perturbation is a superposition of different poloidal harmonics in a tokamak plasma. The neighboring harmonics are linearly coupled and overlapped due to the toroidicity of the configuration. The mode correlation length Δr may be much longer than and independent of the mode width of a single harmonic if such coupling and overlapping are strong. Based on such physical considerations, theoretical studies have shown that radial correlation length can be a function of plasma parameters, independent of and much longer than the mode width of a single harmonic.[16,17] In addition, density fluctuation measurements in tokamak plasmas indicate that the wave number spectrum $S(k_r)$ peaks at $k_r = 0$ while the spectrum $S(k_\theta)$ peaks at $k_\theta \neq 0$.[18] However, finding out the proper formula for Δ_r is still a challenge to plasma physicists and is beyond the scope of this work.

It is qualitatively demonstrated in Sec. III that the ITG mode has the highest maximum growth rate and widest unstable k_θ spectrum in a hydrogen plasma, the lowest maximum growth rate and narrowest k_θ spectrum in a tritium plasma, and the intermediate growth rate and k_θ spectrum in a deuterium plasma. There are uncertainties in the scaling of the radial correlation length with the ion mass number as discussed above. On the other hand, it is reasonable to believe that the growth rate of the mode determines the driving force for the turbulent energy. Based on such argument we assume that the correlation time is determined by the single harmonic with the maximum growth rate and that the correlation length is in-

dependent of the mode width of each single harmonic and determined by equilibrium plasma parameters in an attempt to find a possible relation between these numerical results and the isotope scaling of energy confinement time $\tau_E \propto M_i^{1/2}$ experimentally observed. Under this assumption, the plasma thermal conductivity has the same scaling as the maximum growth rate of the mode does. Keeping this in mind, we discuss the isotope scaling of the maximum growth rate of the mode $\gamma_{\max}$ in the following.

Shown in Fig. 4 is the maximum growth rate from Figs. 1–2 as a function of effective mass number

$$M_{\text{eff}} = (1 - f_z)M_i + f_z M_z \ , \tag{5}$$

where M_i and M_z are the mass number for hydrogenic ions and impurity ions, respectively, and the same normalization as that in Figs. 1 and 2 is used for $\gamma_{\max}$. The solid line is the curve of $\gamma_{\max} \propto M_{\text{eff}}^{-0.5}$ matching to the calculated value at the point $M_{\text{eff}} = 1$. Considering that the parameter values used in the calculation are chosen randomly from that close to experimental observations, the fitting result is considered good.

Shown in Fig. 5 is the same as that in Fig. 4 but for the impurity driven mode. In this case the fitting with $M_i^{-0.5}$, with M_i being the mass number of the hydrogenic ions, is also good. Our attempt to fit these data by one curve with the effective mass number M_{eff} as that for ITG mode failed, indicating that Z_{eff} is important for the maximum growth rate of the impurity mode. Taking the influence of Z_{eff} into account, we find that $\gamma_{\max} \propto M^{-0.5} Z_{\text{eff}}^{1.5}$ fits the data given in Fig. 5 reasonably well. Both ITG and impurity mode have approximately the same isotope scaling $\gamma_{\max} \propto M^{-0.5}$. Furthermore, impurity mode has scaling $\gamma_{\max} \propto Z_{\text{eff}}^{1.5}$ which may provide a way to distinguish impurity mode dominated transport from ITG mode induced transport.

V. CONCLUSIONS

The integral toroidal gyrokinetic dispersion equation is extended to include a second ion species. The ion temperature gradient driven mode (or η_i mode) is studied in hydrogen, deuterium or tritium plasmas with or without the presence of impurity ions. It is shown that the ITG mode has the highest maximum growth rate and the widest unstable k_θ spectrum in a hydrogen plasma, the lowest maximum growth rate and narrowest k_θ spectrum in a tritium plasma, and an intermediate maximum growth rate and k_θ spectrum in a deuterium plasma. The maximum growth rate of the mode with respect to the poloidal mode number k_θ is found to scale as $\gamma_{\max} \propto M_{\text{eff}}^{-0.5}$ with M_{eff} being the effective ion mass number defined in Eq. (5). A possible correlation between this scaling and the experimental observations for plasma energy confinement is discussed with the mixing length estimation under the assumption that correlation time is inversely proportional to the maximum growth rate of the mode and that correlation length is independent of each single harmonic mode width.

The impurity driven mode is studied in hydrogen, deuterium or tritium plasmas without temperature gradient of both primary and impurity ion species. The mode maximum growth rate has the same feature as that of the η_i mode: the highest maximum growth rate and the widest unstable k_θ spectrum in a hydrogen plasma, the lowest maximum growth rate and narrowest k_θ spectrum in a tritium plasma, and an intermediate maximum growth rate and k_θ spectrum in a deuterium plasma. The maximum mode growth rate scales as $\gamma_{\max} \propto M^{-0.5}$ for the same impurity concentration f_z, where M is the mass number of the primary ion species. Taking Z_{eff} into account, $\gamma_{\max} \propto M^{-0.5} Z_{\text{eff}}^{1.5}$ fits the numerical data reasonably well. The scaling $\gamma_{\max} \propto Z_{\text{eff}}^{1.5}$ of the impurity mode is one of the major differences from ITG mode. It may provide a distinction between ITG mode dominated and impurity mode dominated transport.

It has to be pointed out that the isotope scaling discussed in this study only works for fixed

plasma parameters such as density and temperature gradients, magnetic and velocity shears, magnetic curvature and safety factors. This means that the isotope scaling $\gamma_{\max} \propto M_{\text{eff}}^{-0.5}$ proposed in this work only holds for discharges with exactly the same plasma parameter profiles in different working gases. The profiles of those plasma parameters, however, usually change from one working gas to another in experiment. As a result, it is not surprising to find out that weak or even no isotope effects are observed for some plasmas in certain discharge modes as, for example, the L-mode plasmas on Doublet III-D (DIII-D) with neutral beam injection.[19]

ACKNOWLEDGMENTS

This work was supported by the U.S. Department of Energy contract DE-FG05-80ET-53088 and in part by a DOE Fusion Postdoctoral Fellowship administered by the Oak Ridge Institute for Science Education.

REFERENCES

1. R.J. Goldston, Plasma Phys. Contr. Fusion **26**, 87 (1984).

2. S.M. Kaye, Phys. Fluids **28**, 2327 (1985).

3. M. Bessenrodt-Weberpals, F. Wagner, ASDEX Team, Nucl. Fusion **33**, 1205 (1993).

4. R.R. Dominguez, Nucl. Fusion **31**, 2063 (1991).

5. B. Coppi, in Proceedings of the 13th International Conference on Plasma Physics and Controlled Nuclear Fusion Research (International Atomic Energy Agency, Vienna, 1991), Vol. 2, p. 413.

6. B. Coppi, P. Detragiache, S. Migliuolo, M. Nassi, B. Rogers, L. Sugiyama, and L. Zakharov, in Proceedings of the 14th International Conference on Plasma Physics and Controlled Nuclear Fusion Research (International Atomic Energy Agency, Vienna, 1993), Vol. 2, p. 131.

7. B.D. Scott, Phys. Fluids B **4**, 2468 (1992).

8. J.Q. Dong, W. Horton, and X.N. Su, in *AIP Conference Proceedings 284, U.S.-Japan Workshop on Ion Temperature Gradient-Driven Turbulent Transport*, Austin, Texas, 1993, edited by W. Horton, A. Wootton, and M. Wakatani (American Institute of Physics, New York, 1994), p. 486.

9. J.Q. Dong, W. Horton, and J.Y. Kim, Phys. Fluids B **4**, 1867 (1992).

10. B. Coppi, H.P. Furth, M.N. Rosenbluth, and R.Z. Sagdeev, Phys. Rev. Lett. **17**, 337 (1966).

11. W. Horton, D. Lindberg, J.Y. Kim, J.Q. Dong, G.W. Hammett, S.D. Scott, and M.C. Zarnstoff, Phys. Fluids B **4**, 952 (1992).

12. A.D. Beklemishev and W. Horton, Phys. Fluids B **4**, 2176 (1992).

13. T. Tajima, Y. Kishimoto, M.J. Lebrun, M.G. Gray, J.Y. Kim, W. Horton, H.V. Wong, and M. Kotschenreuther, in *AIP Conference Proceedings 284, U.S.-Japan Workshop on Ion Temperature Gradient-Driven Turbulent Transport*, Austin, Texas, 1993, edited by W. Horton, A. Wootton, and M. Wakatani (American Institute of Physics, New York, 1994), p. 255; and M.J. Lebrun, T. Tajima, M.G. Gray, G. Furnish, and W. Horton, Phys. Fluids B **5**, 752 (1993).

14. S.E. Parker, W.W. Lee, and R.A. Santoro, Phys. Rev. Lett. **71**, 2042 (1993).

15. W.M. Tang and G. Rewoldt, Phys. Fluids B **5**, 2451 (1993).

16. J.W. Connor, J.B. Taylor, and H.R. Welson, Phys. Rev. Lett. **70**, 1803 (1993); and J.B. Taylor, J.W. Connor, and H.R. Wilson, Plasma Phys. Contr. Fusion **35**, 1063 (1993).

17. F. Romanelli and F. Zonca, Phys. Fluids B **5**, 4081 (1993).

18. R.J. Fonk, G. Cosby, R.D. Durst, S.F. Paul, N. Bretz, S Scott, E. Synakowski, and G. Taylor, Phys. Rev. Lett. **70**, 3736 (1993).

19. D.P. Schissel, K.H. Burrell, J.C. DeBoo, R.J. Groebner, A.G. Kellman, N. Ohyabu, T.H. Osborne, M. Shimada, R.T. Snider, R.D. Stambaugh, T.S. Taylor, and DIII-D Research Team, Nucl. Fusion **29**, 185 (1989).

FIGURE CAPTIONS

1. Normalized ITG mode growth rate versus poloidal wavenumber for pure hydrogenic plasmas. In all figures the growth rate is in unit of $T_e/\sqrt{2T_i m_H} L_{ne}$, and the wavenumber is in unit of $eB/c\sqrt{2T_i m_H}$.

2. Normalized ITG mode growth rate versus poloidal wavenumber for plasmas with impurities, the solid lines are for helium impurity and the dotted lines for carbon impurity.

3. Normalized impurity mode growth rate versus poloidal wavenumber, (a) $f_z = 0.2$, and (b) $f_z = 0.3$ with oxygen as the impurity.

4. The maximum growth rate of the ITG mode versus the effective mass number for the calculations given in Figs. 1 and 2. The solid line is $\gamma_{\max} \sim M_{\text{eff}}^{-0.5}$ fitting.

5. The maximum growth rate of the impurity mode versus the mass number of the primary ions for the calculations given in Fig. 3 The lines are $\gamma_{\max} \sim M_i^{-0.5}$ fitting, the solid line is for $f_z = 0.2$ and the dash-dotted line for $f_z = 0.3$ with oxygen as the impurity.

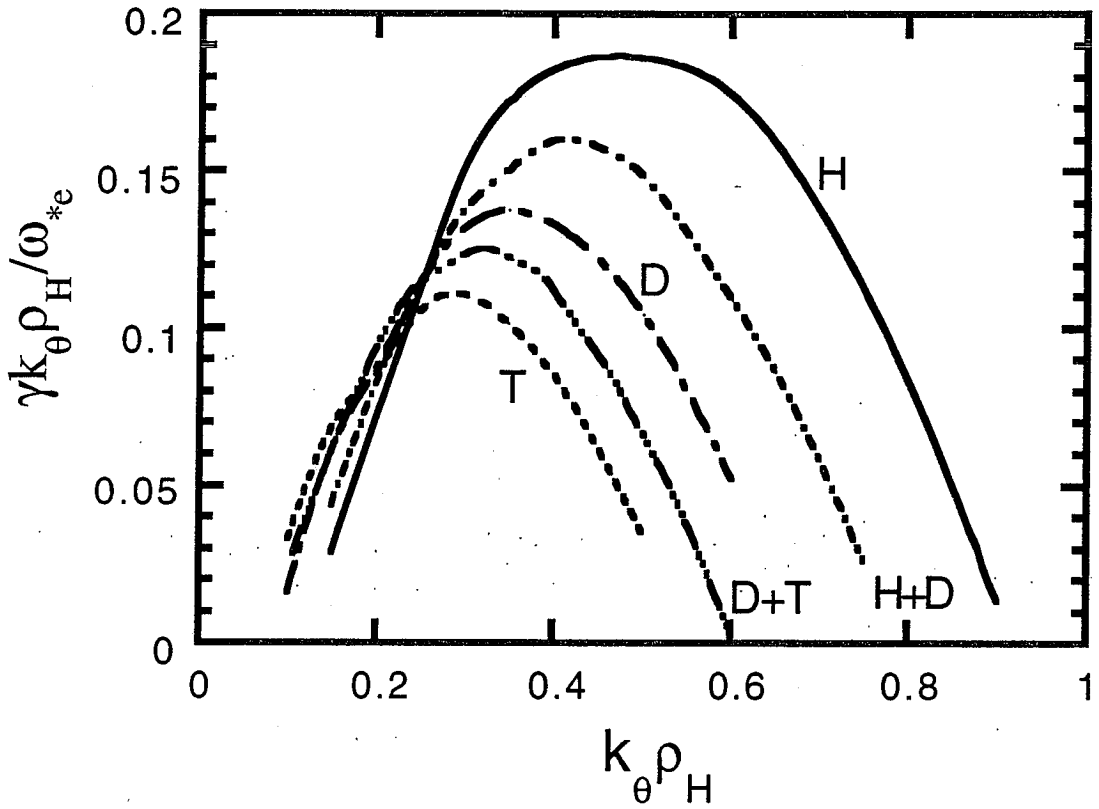
0.2
0.15
0.1
0.05
0
0
0.2
0.4
0.6
0.8
1
$\gamma k_\theta \rho_H / \omega_{*e}$
$k_\theta \rho_H$
H
D
T
D+T
H+D

Fig.1

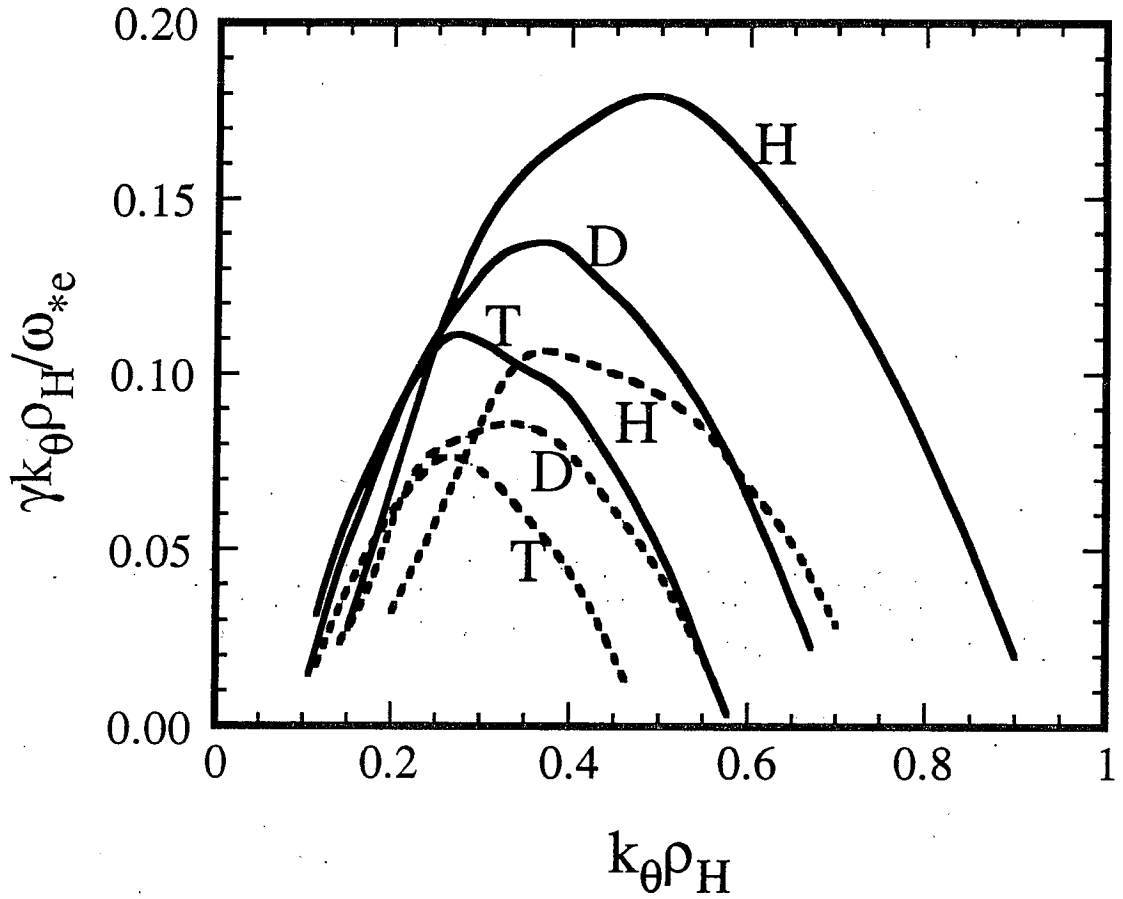
0.20
0.15
0.10
0.05
0.00
0
0.2
0.4
0.6
0.8
1
H
D
T
H
D
T
$\gamma k_\theta \rho_H / \omega_{*e}$
$k_\theta \rho_H$

Fig. 2

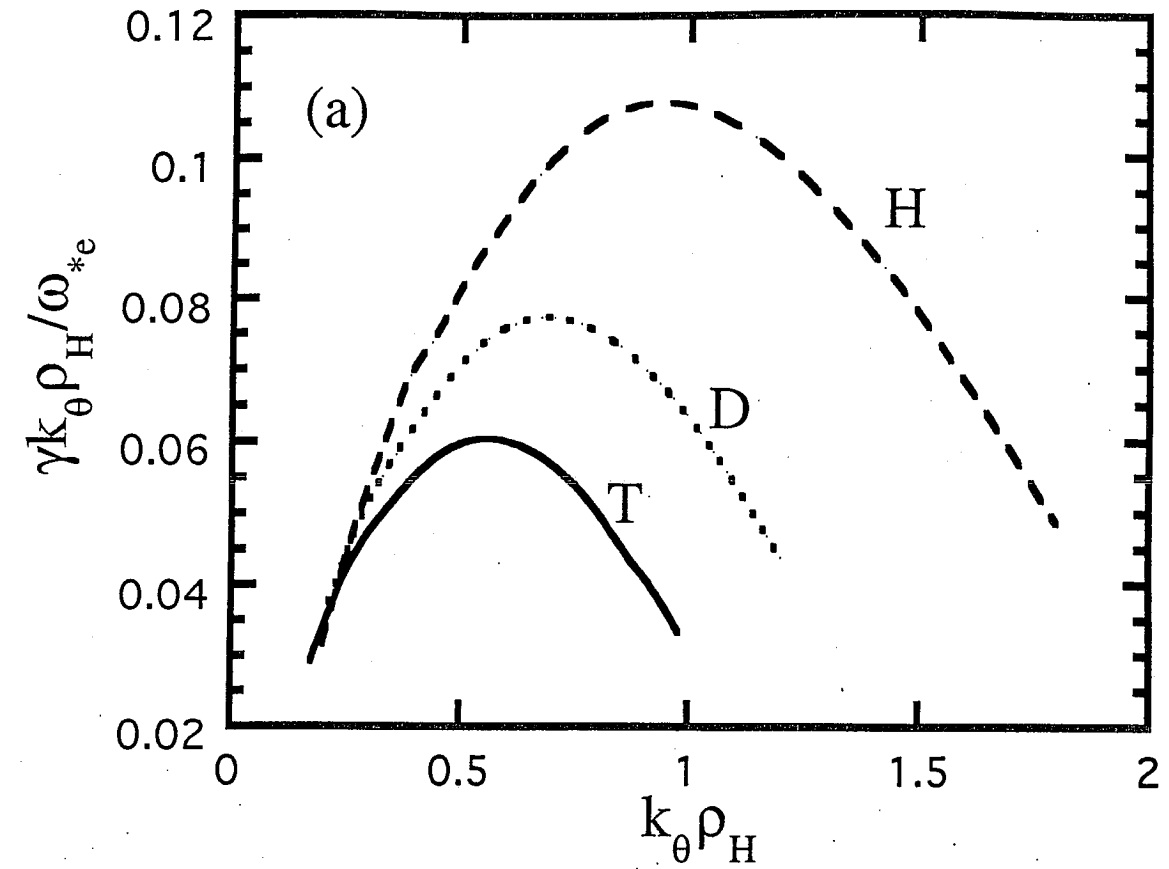
(a)
H
D
T
0.12
0.1
0.08
0.06
0.04
0.02
0
0.5
1
1.5
2
$\gamma k_\theta \rho_H / \omega_{*e}$
$k_\theta \rho_H$

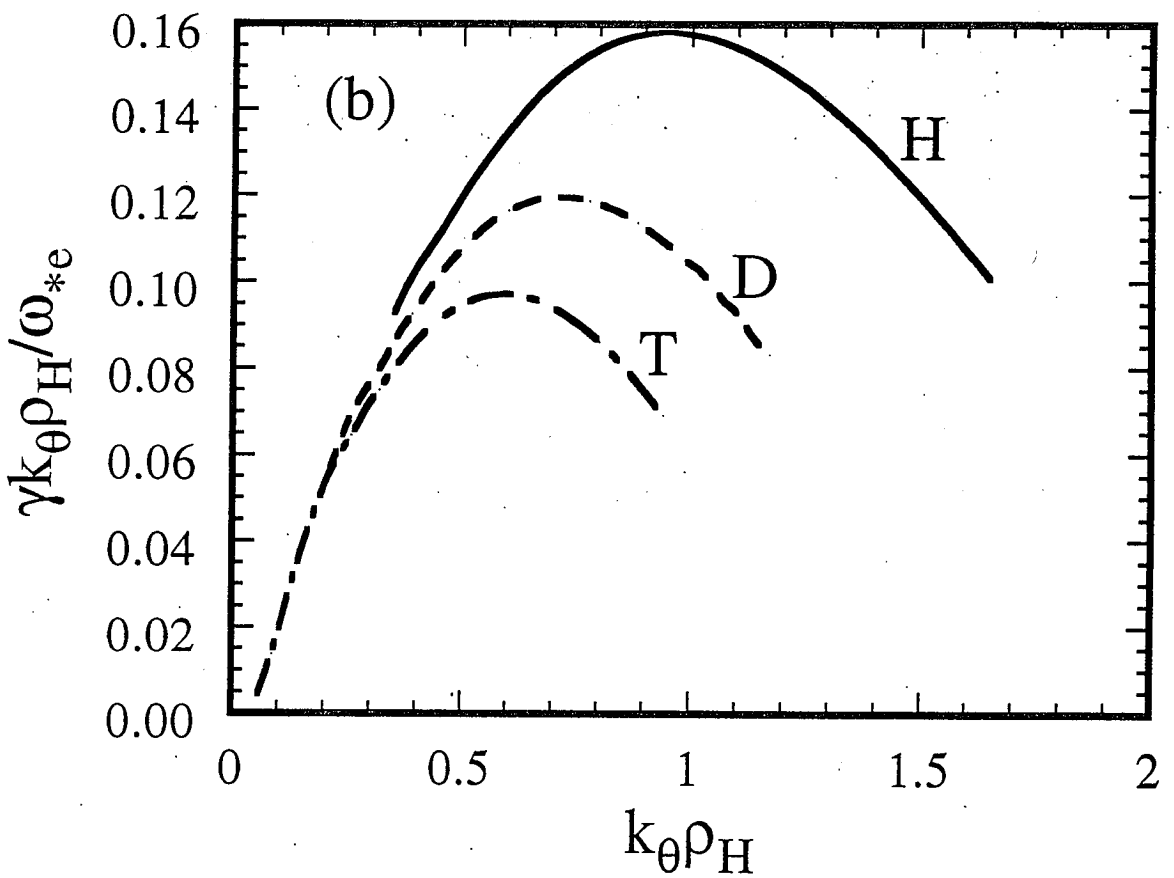
(b)
H
D
T
0.16
0.14
0.12
0.10
0.08
0.06
0.04
0.02
0.00
0
0.5
1
1.5
2
$\gamma k_\theta \rho_H / \omega_{*e}$
$k_\theta \rho_H$

Fig. 3

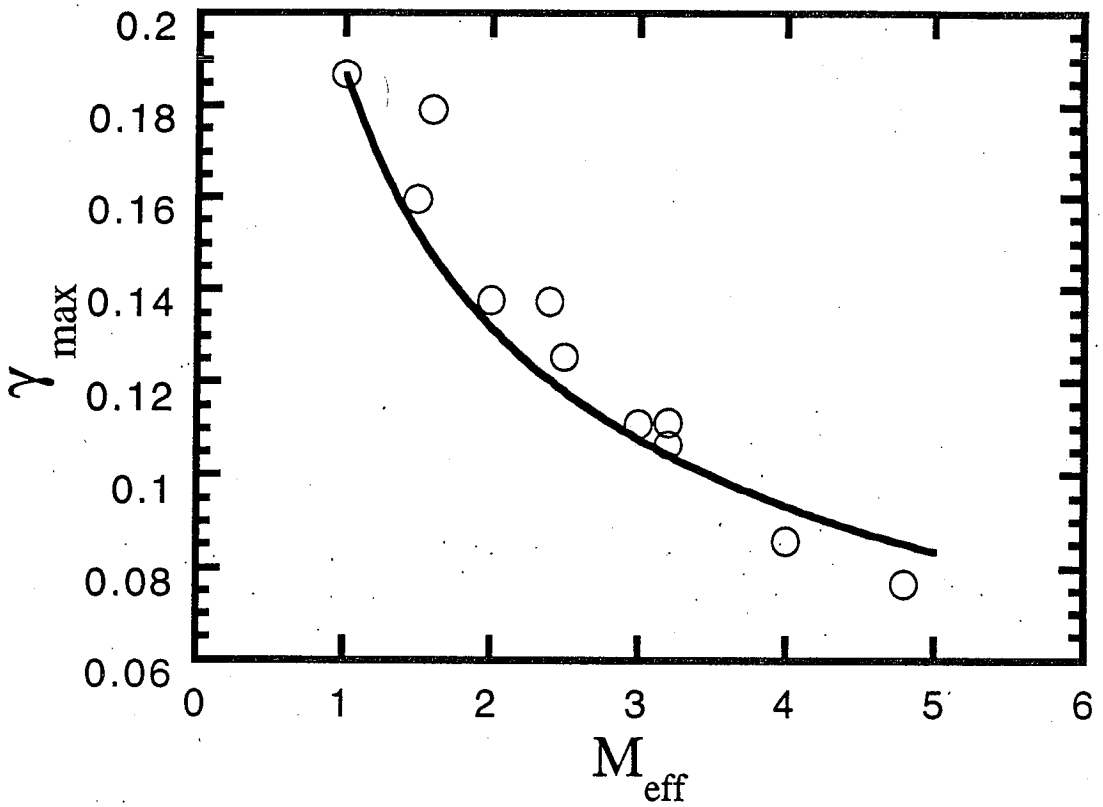

Fig.4

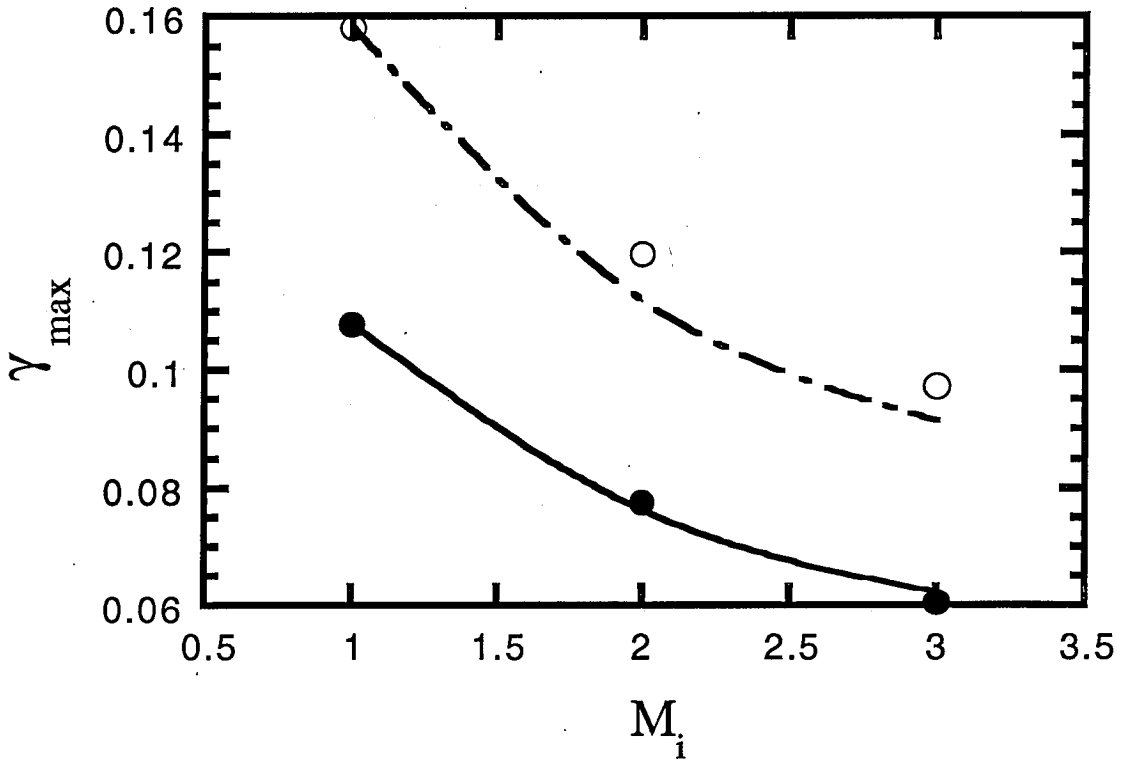

Fig. 5